Biomimetic coatings on titanium: a crystal growth study of octacalcium phosphate

F. BARRÈRE[1,2*], P. LAYROLLE[1], C.A. VAN BLITTERSWIJK[1,2], K. DE GROOT[1,3]
[1]*IsoTis B.V., Prof. Bronkhorstlaan 10, 3723 MB Bilthoven, The Netherlands*
[2]*iBME, Twente University, The Netherlands*
[3]*BRG, Leiden University, The Netherlands*
E-mail: florence.barrere@isotis.com

The biomimetic approach allows the coating of metal implants with different calcium-phosphate (Ca-P) phases. Films elaborated at physiological conditions exhibited structures closely resembling those of bone mineral. For instance, octacalcium phosphate (OCP, $Ca_8(HPO_4)_2(PO_4)_4 \cdot 5H_2O$) crystals have been deposited on titanium through a two-step procedure. After cleaning and etching, Ti6Al4V plates were immersed for 24 h into a simulated body fluid (SBF1). A thin amorphous carbonated Ca-P layer precipitated on the metal substrate. Secondly, these thinly Ca-P coated titanium substrates were immersed for 48 h into another simulated body fluid (SBF2). The thin amorphous carbonated Ca-P layer induced the fast precipitation of a second Ca-P layer of 55 μm in thickness composed of OCP crystals. The measurements of Ca and P concentrations versus soaking time in SBF2 showed that the carbonated Ca-P layer partially dissolved before the deposition of the OCP coating. X-ray diffraction (XRD) revealed that OCP crystals grew epitaxially on the substrate. OCP is known to be one of the precursors during the bone mineralization process, thereby, this new generation of biomimetic coatings are promising for orthopedic surgery.

1. Introduction

Hydroxylapatite (HA) and related calcium-phosphate (Ca-P) ceramics have been widely used in medicine because of their favorable biocompatibility and osteoconductive properties. However, these bioceramics have disadvantages such as difficulty in shaping and low mechanical properties. Many studies have been conducted using Ca-P coatings on metal implants to combine the biocompability of ceramics with the excellent strength of metals. HA plasma-sprayed coating on titanium prostheses is successfully used for joint reconstruction [1]. However, the plasma-spraying technique presents several drawbacks. For instance, (1) it is not possible to evenly deposit HA coating on porous implants and (2) it is not possible to process many Ca-P phases, like octacalcium phosphate (OCP, $Ca_8(HPO_4)_2(PO_4)_4 \cdot 5H_2O$) because they decompose at high temperature. Recently, a biomimetic approach for coating metal implants with Ca-P has been developed [2–4]. This method consists of soaking metal implants into supersaturated Ca-P solutions at physiological pH and temperature. Bone-like apatite films have been deposited on chemically treated titanium surfaces [5–7], by soaking into simulated body fluids (SBFs) over a long soaking time. These thin films were less than 4 μm in thickness. Although HA coatings have been widely applied to titanium, OCP might be also considered for coating metal implants by a biomimetic approach. Indeed, OCP has been identified as one of the Ca-P that participates in the early stage of biomineralization of calcified tissues [8, 9]. The biodegradability and osteoconductivity of OCP have been demonstrated *in vivo* [10, 11]. The aim of this work is first to deposit a biomimetic OCP coating within a two-step procedure by immersing into two different supersaturated Ca-P solutions under physiological conditions; secondly to study the nucleation and growth of the OCP coating on the Ti6Al4V substrate.

2. Materials and methods

2.1. Materials

Plates ($10 \times 10 \times 1\,mm^3$) were cut from a Ti6Al4V sheet (Smitford Staal BV, The Netherlands). The plates were ultrasonically cleaned for 15 min in acetone, then ethanol (70%) and finally demineralized water, respectively. The samples were subsequently etched for 10 min in Kroll's reagent: a mixture of 2 ml hydrofluoric acid (40%), 4 ml nitric acid (66%) and 994 ml of demineralized water. After etching, the Ti6Al4V plates were thoroughly washed with demineralized water.

2.2. Preparation of the biomimetic Ca-P coating

The biomimetic calcium phosphate coatings were produced in two steps as previously mentioned [12].

*Author for correspondence.

The Ti6Al4V plates were first soaked into a solution (SBF1) in order to pretreat the Ti6Al4V substrate with Ca-P nuclei. Later, the samples were immersed into a second solution (SBF2) in order to grow the biomimetic coating.

2.2.1. Soaking of Ti6Al4V plates into SBF1

SBF1 was prepared by dissolving NaCl, $CaCl_2 \cdot 2H_2O$, $MgCl_2 \cdot 6H_2O$, $NaHCO_3$ and $Na_2HPO_4 \cdot 2H_2O$ salts into demineralized water under mildly acidic conditions. All the chemicals have been weighted with a confidential interval of 10 mg. This solution was prepared with reagent pure chemicals (Merck). The plates were soaked into the first solution SBF1 for 24 h at 37 °C. The preparation of SBF1 is mentioned elsewhere [4].

2.2.2. Soaking of seeded Ti6Al4V plates into SBF2

SBF2 was prepared by dissolving NaCl, $CaCl_2 \cdot 2H_2O$ and $Na_2HPO_4 \cdot 2H_2O$ salts into demineralized water. Crystal growth inhibitors, such as Mg^{2+} and HCO_3^{2-}, were excluded from SBF2 solution, while the ionic strength was kept constant by adding NaCl. This solution was prepared with reagent pure chemicals (Merck). SBF2 solution was buffered at pH = 7.05 at 37 °C by adding a mixture of tris-hydroxymethylaminomethane (TRIS, 50 mM) and 1 M HCl. All the chemicals have been weighted with a confidential interval of 10 mg. Finally the solution was filtrated through a 0.22 μm Millipore membrane. Subsequently to pretreatment in SBF1, the plates were immersed into the second solution (SBF2) for 48 h at 37 °C. As control, two etched Ti6Al4V plates were immersed into SBF2 solution without previous pretreatment into SBF1 solution.

2.3. Kinetic study

The kinetic study is based on the characterization of the coating as well as the composition of SBF2 versus soaking time. The experiments have been repeated 5 times.

2.3.1. Analyses of the coating versus soaking time

Twenty seeded Ti6Al4V samples were individually and vertically placed in polystyrene vials containing 60 ml of SBF2 solution. The vials were sealed and put in a calibrated shaking water-bath at 37 °C. For each sampling time (1, 2, 3, 4, 5, 6, 7, 8, 12, 24 and 48 h of soaking), two soaked plates were taken out from SBF2. The samples were subsequently cleaned with demineralized water and dried overnight in air. The coating morphology was observed by environmental scanning electronic microscopy with field emission gun (ESEM, Philips, model XL-30 ESEM-FEG) coupled with energy dispersive for X-ray analysis (EDX, Philips). The coating thickness has been determined by using a magnetic induction probe (Electrophysik, Minitest 2100, Germany). The measuring range of this apparatus is between 0 and 100 μm. The probe was calibrated with standard polymer films 10 μm thick on a Ti6Al4V plate etched and cleaned in the same conditions as the other samples. The measurements were repeated 10 times on each sample. For every Ca-P coated plates, the thickness value was determined by averaging the data. The structure was determined by Fourier Transform InfraRed spectrometry (FT-IR, Perkin-Elmer, Spectrum 1000) using transparent KBr pellets of 250 mg and containing 1 mg of Ca-P coating. An X-Ray diffractometer (XRD, Philips, model APDW40C) rebuilt for thin-film (TF) applications was used to determine the crystal phase of Ca-P deposited on Ti6Al4V. The monochromatic source was a Cu generator (40 kV, 50 mA) and TF-XRD were patterned for raising angles $3° < 2\theta < 60°$ with a step size of 0.5°.

2.3.2. Analyses of SBF2 versus soaking time

Two treated Ti6Al4V samples were individually and vertically placed in polystyrene vials containing 60 ml of SBF2 solution. The vials were sealed and put in a calibrated shaking water-bath at 37 °C for 48 h. For comparison, a SBF2 control vial without a Ti6Al4V plate was placed in the mean time under similar conditions. A sampling from each vials of 1 ml of SBF2 solution was performed after 1, 2, 3, 4, 5, 6, 7, 8, 12, 24 and 48 h of soaking. The pH of SBF2 solution was measured in the same conditions after calibration with 2 buffer solutions pH = 4.01 and pH = 7.00 (IUPAC standards, Radiometer Copenhagen). A combined pH electrode (Portamess 913, Knick Eletctronische Messgerate, Holland) was used. The calcium concentrations [Ca] in SBF2 solutions were measured by atomic absorption spectroscopy (AAS, Varian SpectrAA-300, Australia). Standard solutions were made by diluting 1000 ppm Ca stock solution with demineralized water to a level of 20, 40, 60, 80 and 100 ppm. A $LaCl_3$ solution (about 0.6 vol %) was used as a releasing agent to eliminate the depression of Ca absorption by the acetylene flame. Both the standard and sample solution (0.1 ml of each) were diluted with 3.0 ml of the lanthanum solution and then analyzed. The measurements were done in triplicate for each standard and sample solutions. The phosphorus concentrations [P] were determined by spectrophotometry of a phosphomolybdate complex at 820 nm (Vitalab 21, Vital scientific, Holland). Standard solutions were made by diluting 1000 ppm P-stock solution with demineralized water to a level of 50 and 100 ppm. Measurement

TABLE I Inorganic composition (mM) of Human Blood Plasma (HBP), and Simulated Body Fluids (SBF)

	Na^+	Mg^{2+}	Ca^{2+}	Cl^-	HPO_4^{2-}	HCO_3^{2-}
HBP	142.0	1.5	2.5	103.0	1.0	27.0
SBF1	733.5	7.5	12.5	720.0	5.0	21.0
SBF2	140.4	—	4.0	142.9	2.0	—

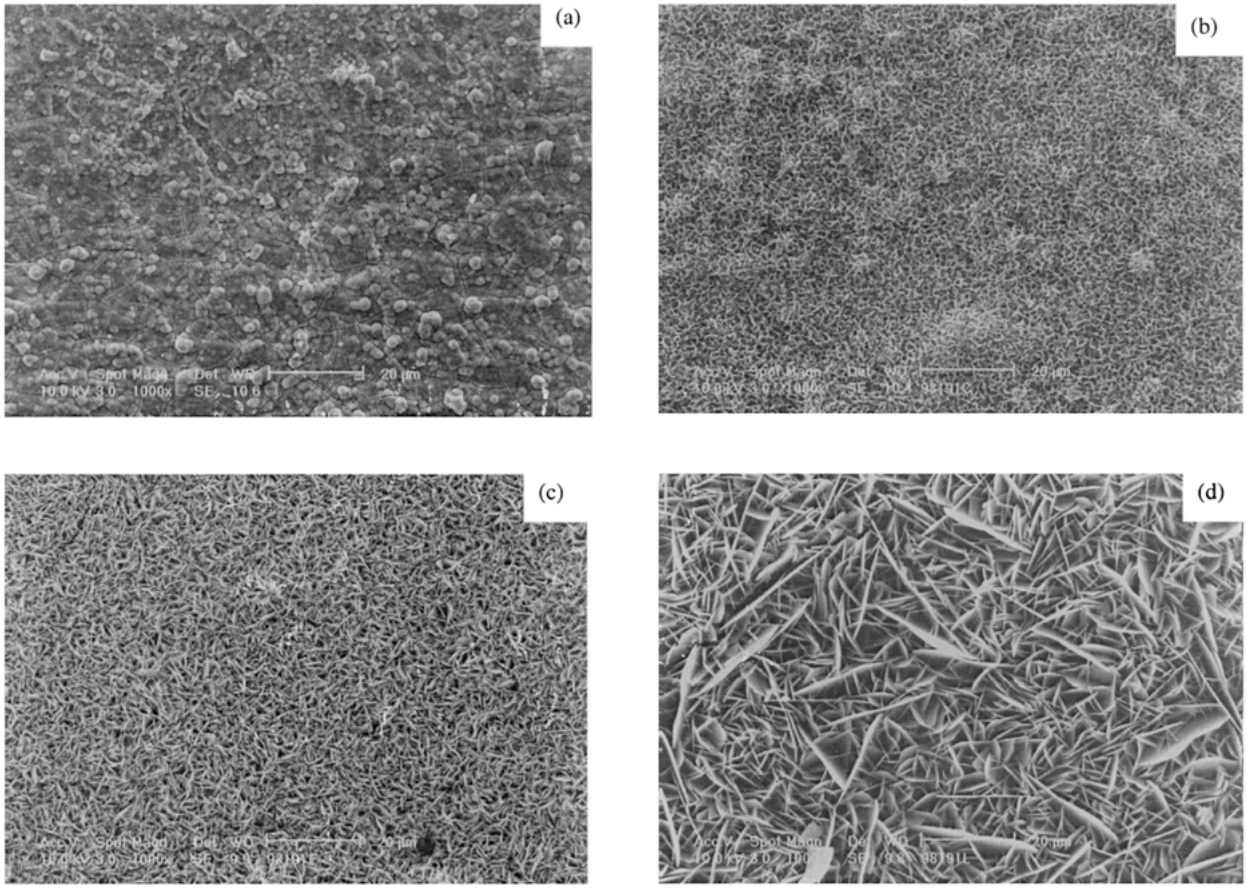

Figure 1 Morphology evolution of the Ca–P coating versus soaking time: (a) pretreated surface; (b) after 2 h of soaking; (c) after 5 h of soaking; (d) after 48 h of soaking.

involved 0.1 ml of each solution, including the P standards, with 7 ml of ammonium molybdate acidified with condensed sulfuric acid in the presence of ascorbic acid. After the mixed solutions have been kept at 37 °C for 90 min, a blue color (molybdene blue) developed. The blue solutions were vortexed and the phosphate concentration [P] was determined after calibration with the standard solutions. The optical density of the complex was measured 3 times.

3. Results

3.1. Analyses of the coating versus soaking time

After 24 h of pretreatment into SBF1, ESEM and EDX observations indicated that a dense and uniform Ca-P film was deposited on the Ti6Al4V plates (Fig. 1(a)). This layer is composed of spherical Ca-P globules of about 0.1 µm in diameter. After soaking into SBF2 solution, no coating was deposited on the non-pretreated Ti6Al4V plates whereas Ca-P coatings were detected on the pretreated plates in SBF1 solution. After soaking for 2 h in SBF2 solution, the initial Ca-P film has already changed in morphology. Ca-P globules have increased in size and are covered by small crystals of less than 5 µm in length (Fig. 1(b)). As soaking time increased, these crystals appeared larger and the globules were no more visible. After 48 h of soaking, these sharp crystal plates were approximately 30 µm in length and 0.1 µm in thickness. The crystalline coating covered uniformly the surface of Ti6Al4V plates. During the whole experiments, any homogeneous precipitation did not occurred in SBF2 solution. As shown in Fig. 2, the Ca-P layer became thicker as the soaking time increased. The thickness curve plotted versus the logarithm of soaking time exhibits an hyperbolic shape. After 48 h of soaking into SBF2 solution the coating had a thickness of 55 µm. FTIR spectra of the coating are gathered in Fig. 3. As the soaking time evolved, the structure of coating changed. Initially, the FTIR spectrum of the seeded Ti6Al4V substrate after soaking into SBF1 (Fig. 3(a)) showed

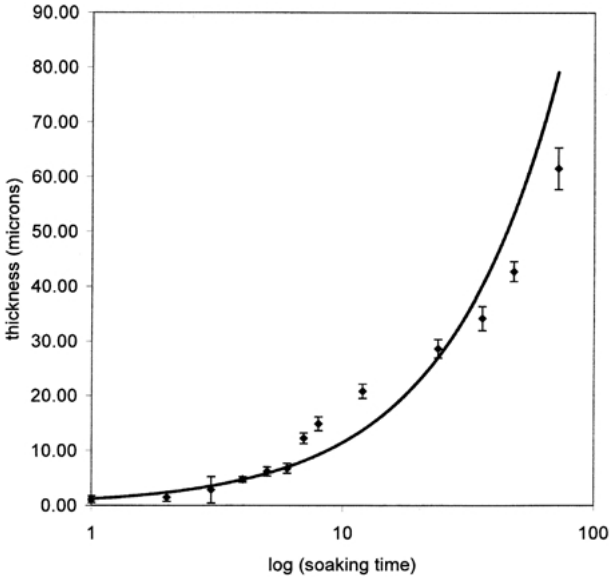

Figure 2 Ca–P coating thickness versus soaking time.

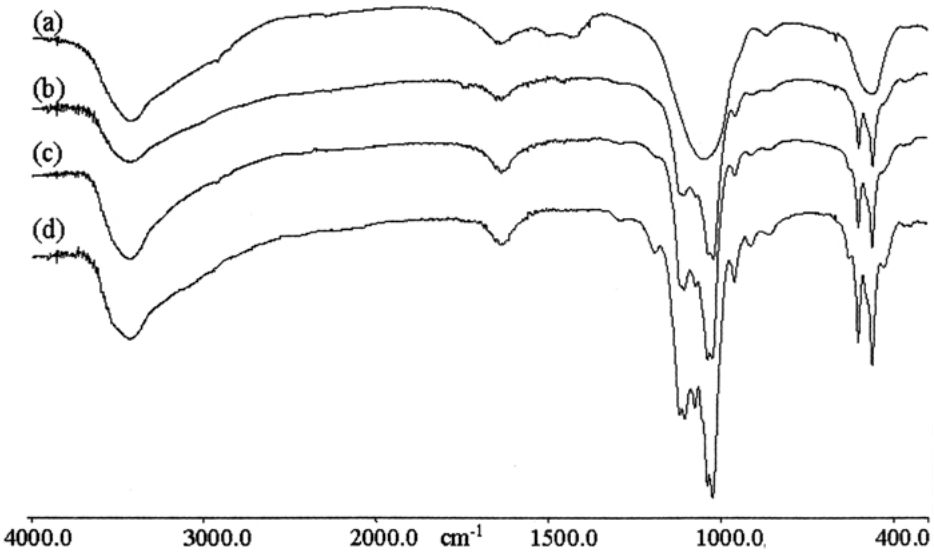

Figure 3 FTIR spectra of the coating, structure evolution versus soaking time: (a) pretreated surface; (b) after 2 h of soaking; (c) after 5 h of soaking; (d) after 48 h of soaking.

featureless phosphate and carbonate bands. Phosphate groups exhibited broad and single bands at 560 cm^{-1} (P-O deformation in $PO_4(\nu_4)$) and 1041 cm^{-1} (P-O stretching in $PO_4(\nu_3)$). The carbonate bands were also observed at 1410 and 1450 cm^{-1}. The spectrum of the Ca-P film is typical of an amorphous carbonated calcium phosphate. For 2 h soaking, FTIR spectrum (Fig. 3(b)) exhibits a mixture of 2 phases. The single large P-O band at 560 cm^{-1} evolved to sharp bands at 560 and 600 cm^{-1}, respectively. The broad and single P-O band at 1041 cm^{-1} exhibited a fine structure with vibrations and shoulders at 1025 and 1011 cm^{-1}. The coating appeared more crystalline. Moreover new bands appeared at 906 and 852 cm^{-1}, which are typical of HPO_4^{2-} bands in OCP structure [13]. The OCP phase appeared predominant and unique after 48 h of soaking into SBF2 (Fig. 3c and d). The XRD patterns (Fig. 4) corroborate the previous results obtained by FTIR spectroscopy. The pretreated Ti6Al4V surface pattern (Fig. 4(a)) showed a halo or bump located at approximately 30° typical of a Ca-P amorphous state.

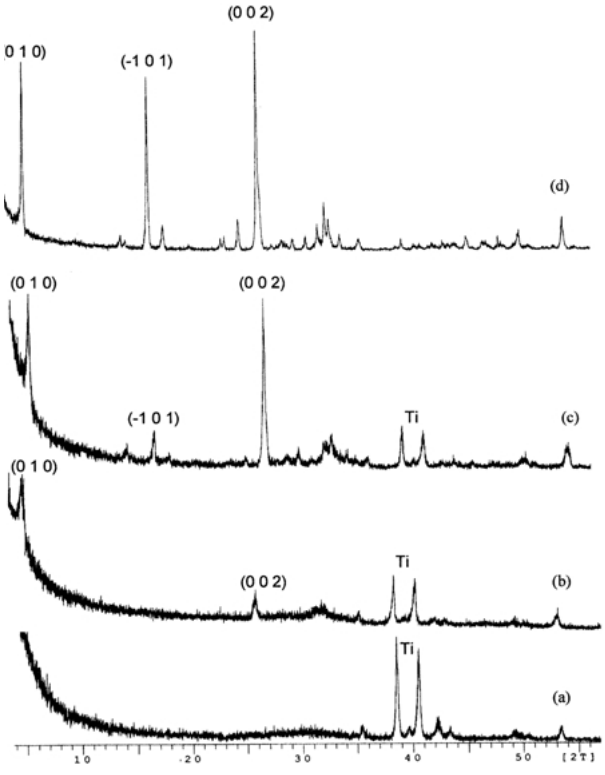

Figure 4 XRD characterization: Crystal features of the coating versus soaking time: (a) pretreated surface; (b) after 2 h of soaking; (c) after 5 h of soaking; (d) after 48 h of soaking.

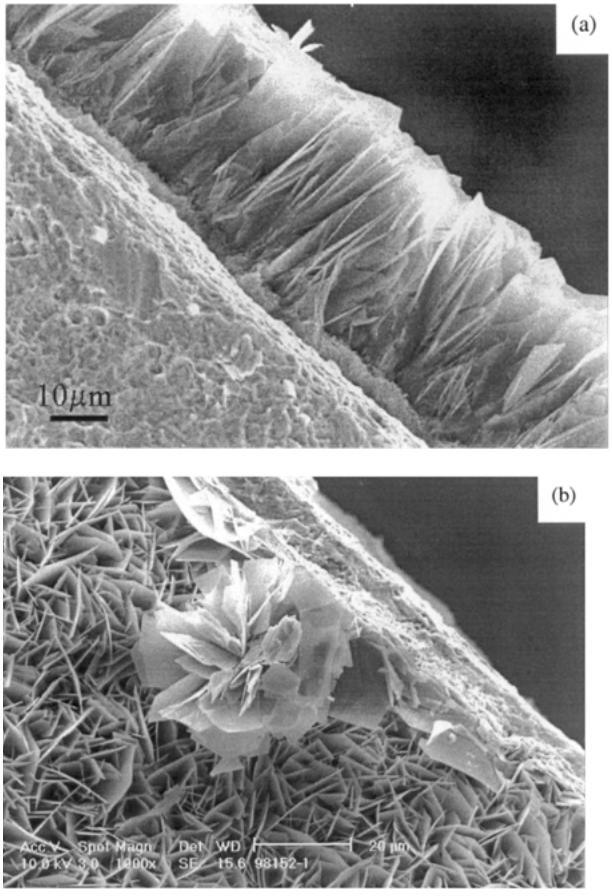

Figure 5 OCP specific crystal growth. (a) OCP crystals growing vertically on the top of the thin amorphous carbonated Ca-P film, (b) primary OCP growth on flat Ti6Al4V substrate and secondary OCP growth with a rose-like shape.

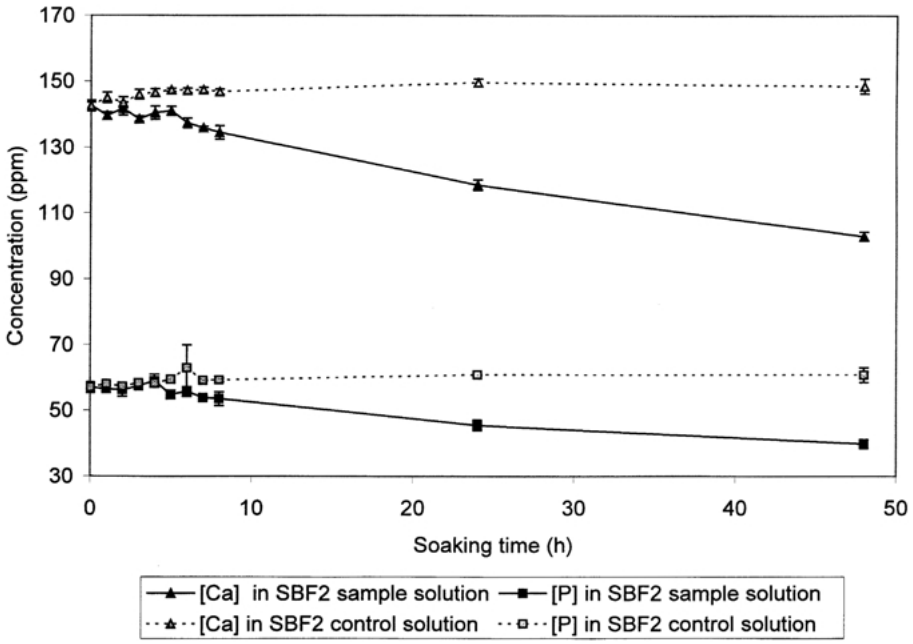

Figure 6 Ca and P concentration in SBF2 solution (sample and control) versus soaking time.

The other sharp peaks at $2\theta = 35.5°$, 38.6°, 39.6°, 40.5° and 42.2° were assigned to the Ti6Al4V substrate. After 2 h of soaking into SBF2 (Fig. 4(b)), additional sharp diffraction lines appeared at $2\theta = 4.7°$ corresponding to (0 1 0) diffraction line and at $2\theta = 25.5°$ corresponding to the (0 0 2) plan, both typical of triclinic OCP crystals [14]. After 5 h of soaking, the diffraction lines of the titanium substrate were less intense as compare to the diffraction peaks related to Ca-P phase decreased (Fig. 4(c) and (d)). Furthermore, a new line appeared at $2\theta = 16.8°$ corresponding to $(-1\,0\,1)$ diffraction in the OCP structure. This indicated that the coating has grown and presents a high crystallinity. However, the relative intensities of the OCP diffraction peaks present mismatches with the typical OCP pattern [14]. Indeed, the diffraction line (0 0 2) has the highest intensity in the XRD-pattern whereas the diffraction line (0 1 0) is the most intense peak for the pattern of typical triclinic OCP crystals. Moreover the diffraction line $(-1\,0\,1)$ at $2\theta = 16.8°$ is much more intense in our OCP coating than the typical triclinic OCP crystals [14]. This suggested that the OCP crystals have grown on the substrate after the favorite directions $(-1\,0\,1)$ and (0 0 2). This specific growth is shown in Fig. 5, where OCP crystals are all perpendicularly oriented to the substrate. Fig. 5(b) exhibited also the vertical crystals growing from the substrate whereas the rose-like OCP crystal on the top of coating spread over all directions. This indicated that the substrate influences the OCP crystal growth.

3.2. Characterization of SBF2 versus soaking time

Fig. 6 shows the concentrations of Calcium [Ca] and Phosphorus [P] in SBF2 solution (control and samples) as a function of soaking time. The composition of the control SBF2 solution remained constant whereas the concentrations in the sample SBF2 solution decreased with soaking time. Calcium and phosphorus concentrations (respectively [Ca] and [P]) graphs versus soaking time showed similar behaviors. [Ca] and [P] in SBF2 solution mainly decreased with the soaking time indicating the deposition of a Ca-P coating. During the first 10 h, an oscillating tendency between uptake and release of Ca and P was observed. Both ions were partially released from the seeded Ti6Al4V surface and Ca-P reprecipitated from the solution. The OCP crystals grew on the top of this Ca-P layer. After soaking for 48 h [Ca] and [P] concentrations were approximately 100 ppm and 40 ppm, respectively. The initial pH of the buffered control SBF2 solution remained at $pH = 7.05$ during the 48 h of soaking at 37 °C. Whereas the pH in the soaking SBF2 solution slightly decreased to $pH = 6.95$ which is characteristic of Ca-P formation.

4. Discussion

The results showed that a calcium phosphate coating of 55 μm in thickness deposited on Ti6Al4V after 48 h of soaking. This layer is composed of pure OCP crystal plates that grow on top of a thin amorphous carbonated Ca-P layer at physiological conditions (Fig. 5(a)). The absence of any Ca-P coating on the 2 control Ti6Al4V plates indicated that this layer was essential to induce precipitation of the Ca-P coating. This first Ca-P film deposited on the Ti6Al4V substrate acted as a seeding surface. OCP crystals grow on the top of the dense seeding Ca-P layer. This formation is a dynamic process involving the partial dissolution of the primary Ca-P film and the reprecipitation of the crystalline phase from SBF2 solution. The supersaturation of SBF2 solution increases at the vicinity of the substrate and thereby leads to the heterogeneous nucleation of Ca-P crystals. The continuous oscillating phenomenon could be due to an Ostwald ripening process of Ca-P nuclei: the smallest seeds dissolve in favor to the biggest seeds. Works on the soaking of Ca-P seeds into supersaturated calcifying

solutions showed that fast changes of the precipitates' phases occurred when the soaking time increase [15, 16]. This suggests that those metastable phases might dissolve before the precipitation of another subsequent Ca-P phase. This could explain the oscillating phenomenon of precipitation–dissolution. However, in our experimental conditions, no intermediates were observed. Furthermore, this oscillating process occurs for about 10 h, while the XRD pattern of the coating obtained after 2 h (Fig. 4) of soaking in SBF2 solution shows already diffraction line (0 1 0) of triclinic OCP crystals. This could indicate a unique deposited phase. It seems that OCP crystals grow directly on the top of the first Ca-P film that dissolves partially in SBF2 solution. When the first Ca-P layer dissolves, it can initiate the deposition of OCP [$Ca_8H_2(PO_4)_6 \cdot 5H_2O$]. Its precipitation resulted in a slight decrease of pH in SBF2. This mechanism can be illustrated by the following equation:

$$8Ca^{2+} + 6HPO_4^{2-} + 5H_2O \rightarrow Ca_8H_2(PO_4)_6 \cdot 5H_2O + 4H^+ \quad (1)$$

Besides the influence of the seeding role of the Ca-P film on the nature of the subsequent Ca-P coating, authors have shown that the formed phase depends on the characteristics of the soaking supersaturated solution [17–20]. Furthermore, several Ca-P phases can precipitate at the same conditions. It has been quite well established that the precipitation of Ca-P obeyed to solubility and kinetics of the different possible phases in the supersaturated solution [20]. Indeed the most soluble product is kinetically favored. In our experimental conditions, SBF2 solution is supersaturated in respect to both HAP and OCP phases. HAP is the most thermodynamically stable Ca-P phase at physiological conditions but OCP is more soluble than HAP thus, OCP is kinetically favored as compared to HAP [21]. Subsequently OCP, being a metastable phase, can be transformed into thermodynamically stable Ca-P phases [15, 20, 22]. For instance, OCP has been detected *in vitro* as an intermediate before the formation of HAP [15, 20]. However, other studies [12, 19, 21] have isolated stable OCP crystals at physiological conditions. In our study, the thick OCP layer is stable while the soaking time is increasing. The OCP coating continuously grows while the supersaturation in SBF2 solution decreases. The crystals appear perpendicularly oriented to the substrate. However, the crystal growth evolves during the coating formation. Firstly, the crystals start to nucleate allover the sample surface at the vicinity of each other. When the pretreated Ti6Al4V plates are soaked into SBF2 solution, OCP crystals start to grow following mainly the (0 1 0) direction (Fig. 4(b)), like regular OCP crystals. They spread allover the substrate with a rose-like shape following the 3 directions as shown in Fig 1(b). Subsequently, OCP crystals grow differently following ($-$1 0 1) and (0 0 2) plans to the detriment to (0 1 0) plan (Fig. 4(c) and (d)). This specific orientation is mainly due to the substrate. The crystals cannot spread anymore on the surface along the *x*- and *y*-axis due to a steric effect. Thereby, OCP crystals are forced to grow only along the *z*-axis, perpendicularly to the substrate (Fig. 5). Substrate influence is illustrated in Fig. 5(b). The OCP crystals grown on the Ti substrate are vertical to the plate whereas the rose-like OCP crystal grown on the top of the primary crystals, can grow freely along all directions.

5. Conclusion

A two-step biomimetic procedure allowed the formation of an OCP coating of 55 μm in thickness. First a thin and amorphous carbonated Ca-P film was uniformly deposited on Ti6Al4V substrate. Subsequently, this film induced the nucleation and growth of OCP crystals with a specific orientation, by soaking into a second solution. The biomimetic approach allowed thereby the formation of a new Ca-P phase as coatings on Ti6Al4V substrate. These Ca-P coatings produced at physiological conditions might enhance biocompatibility and bioactivity of orthopedic implants.

References

1. R. G. T. GEESINK and N. H. M. HOEFNAGELS, *J. Bone Joint Surg*. **77B** (1995) 534.
2. T. KOKUBO, H. KUSHITANI, Y. ABE and T. YAMAMURO, *Bioceramics* **2** (1990) 235.
3. P. LAYROLLE, C. A. VAN BLITTERSWIJK and K. DE GROOT, *Bioceramics* **11** (1998) 465.
4. F. BARRERE, P. LAYROLLE, C. A. VAN BLITTERSWIJK, K. DE GROOT, *Mat. Res. Symp. Proc.* **599** (2000) 135.
5. P. LI, I. KANGANESNIEMI, K. DE GROOT and T. KOKUBO, *J. Am. Ceram. Soc*. **77** (1994) 1307.
6. T. PELTOLA, M. PATSI, H. RAHIALA, I. KANGASNIEMI and A. YLI-URPO, *J. Biomed. Mater. Res.* **41** (1998) 504.
7. P. LI and P. DUCHEYNE, *J. Biomed. Mater. Res.* **41** (1998) 341.
8. R. Z. LEGEROS, in ''Biological and Synthetic Apatites in Hydroxyapatite and Related Materials'' edited by P. W. Brown and B. Constanz (CRC Press, Roca-Batton, 1994) p. 3.
9. W. E. BROWN, *Nature* **196** (1962) 1048.
10. F. SUGIHARA, H. OONISHI, S. KUSHITANI, N. IWAKI, Y. MANDAI, K. MINAMIGAWA, E. TSHUJI, M. YOSHIKAWA and T. TODA, *Bioceramics* **8** (1995) 89.
11. O. SUZUKI, M. NAKAMURA, Y. MIYASAKA, M. KAGAYAMA and M. SAKURAI, *Tohoku J. Exp. Med.* **164** (1991) 37–50.
12. F. BARRERE, P. LAYROLLE, C. A. VAN BLITTERSWIJK and K. DE GROOT, *Bone* **25** (1999) 107S.
13. B. O. FOWLER, M. MARKOVIC and W. E. BROWN, *Chem. Mater* **15** (1993) 1417.
14. Joint Comity for Powder Diffraction Standards, OCP 26-1056 (1992).
15. E. D. EANES and J. L. MEYER, *Calcif. Tiss. Res.* **23** (1977) 259.
16. E. C. MORENO and K. VARUGHESE, *J. Crystal Growth* **53** (1981) 20.
17. R. Z. LEGEROS, R. KIJKOWSKA and J. P. LEGEROS, *Scan. Elec. Micros.* **IV** (1984) 1771.
18. P. T. CHENG and K. P. H. PRITZKER, *Calcif. Tissues Int.* **35** (1983) 596.
19. M. IIJIMA, H. KAMEMIZU, N. WAKAMATSU, T. GOTO, Y. DOI and Y. MORIWAKI, *J. Crystal Growth* **112** (1991) 467.
20. M. J. J. M. VAN KEMENADE and P. L. DE BRUIJN, *J. Colloid Interface Sci.* **118** (1987) 564
21. J. C. HEUGHEBAERT and G. H. NANCOLLAS, *J. Phys. Chem.* **88** (1984) 2478.
22. R. Z. LE GEROS, G. DACULSI, I. ORLY, T. ABERGAS and W. TORRES, *Scan. Micros.* **1** (1989) 129.

Received 13 March
and accepted 28 July 2000